Prediction of the overall behavior of a 3D microstructure of austenitic steel by using FFT numerical scheme

A. Belkhabbaz[a], R. Brenner[a], N. Rupin[b], B. Bacroix[a], J. Fonseca[c]

[a]*Laboratoire des propriétés Mécaniques et Thermodynamiques des Matériaux , CNRS, Institut Galilée , Université Paris Nord , av.J.B Clement , 93430 Villetaneuse , France.*
[b]*Electricité de France , Département Matériaux et Mécanique des composants , les Renardières , 77818 Moret sur loing , France.*
[c]*Manchester Materials Science Centre , The university of Manchester , Grosvenor Street , Manchester M1 7HS , UK.*

Abstract

The present work investigates the mechanical response of a polycrystalline aggregate by the combined use of 3D X-ray diffraction contrast tomography (DCT) experiment and the fast Fourier transform (FFT) numerical homogenisation scheme. The microstructure of a recrystallized sample of 304L austenitic steel has been characterized with the DCT technique at ESRF (ID11 beamline) which allows to have access to the spatial distribution and the individual shape of the constituent grains together with their crystalline orientation. To estimate the mechanical behaviour of such real polycrystalline microstructure, the most widely used approach is based on the finite element technique which implies a tedious and complex task of meshing. To circumvent this difficulty, an attractive approach is the FFT-based numerical scheme which allows to use the digital image of the microstructure as a direct input to compute the mechanical response of a heterogeneous material. The efficiency of this method combined with experimental tomographic data is emphasized and the elastic and elastic-plastic behavior of the polycrystalline sample is investigated. Comparisons are made with estimates delivered by the self-consistent approach, that rely on partial information on the microstructure, and first order bounds.

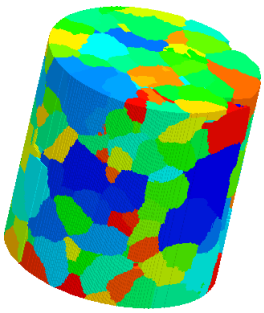
1. Introduction

Some years ago, the only available information to describe the microstructure of a metallic material was based on optical observations, to describe the shape of the grains at the surface of the material and X-ray diffraction, to describe the overall crystallographic texture of the material. During the last decade, important advances have been made with the development of automated EBSD technique [1] which gave rise to orientation imaging microscopy: the orientation and the shape of the grains at the surface of a polycrystal can be characterized. The mechanical modeling of polycrystals now makes use of these microstructural data in order to improve the description of their effective properties [2] and microstructural evolutions [3]. However, the full-field modelling approaches generally require additional assumptions in order to obtain a 3D virtual microstructure from experimental 2D informations [4, 3] and it has been shown that the morphology of the "substrate" strongly influences the fields which can be observed at the surface [5]. A full experimental description of the 3D microstructure is thus necessary but remains difficult to obtain with the EBSD technique since it requires long and tedious treatments of the material (etching or machining) [6]. Even if this technique has been recently improved with the

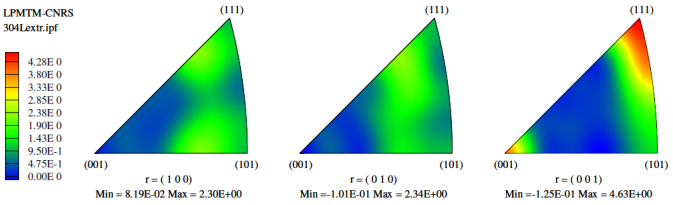
erosion process by focused ion beam (FIB) [7], an inherent limitation of this method is its destructive nature. An alternative technique is the diffraction contrast tomography (DCT) which makes use of X-ray synchrotron radiation to characterize the crystalline orientation and 3D grain shape within the bulk of the polycrystal [8]. These newly experimental informations can serve to model the microstructure either with a statistical decription to enrich homogenization models or with a pointwise description to perform full field simulations. The use of these data for finite element (FE) computations, although possible [9], requires a preliminary complex task of meshing and leads to computations with a huge number of degrees of freedom. In the present work, the alternative method based on fast-Fourier transform (FFT) which has been proposed to overcome these difficulties [10] will thus be preferred.
This article investigates the combined use of DCT data with the FFT numerical scheme to compute efficiently the mechanical response of a real 3D aggregate of 304L stainless steel. The elastic behavior is first studied and compared to the self-consistent estimate and first-order bounds, then some preliminary results are derived for time independent elastoplasticity.

2. DCT technique and 3D microstructure

The DCT [8, 9] allows to capture simultaneously grains shape and orientation in the bulk of a sample. The principle of the method consists in combining 3D reconstruction from projections and diffraction techniques. The diffraction is realized thanks to a parallel, monochromatic beam of synchrotron radiation (ESRF ID11 beamline). The sample is continuously rotated through 360° perpendicularly to the incident beam direction during the illumination. Grains orientation fulfill Bragg conditions several times during the rotation of the sample and then diffracted patterns can be observed on the screen. An algebraic reconstruction technique can be used on these indexed patterns in order to obtain each grain shape, then these constituants are reassembled in the 3D polycrystalline structure.
The limitations of this technique are: it can only be used on small samples (~500μm of diameter) of single phase material with large grains (~20μm), the spatial resolution is of few microns and the angular precision is of 0.1°.
The polycrystal reconstructed by DCT, composed of 362 grains, is displayed on figure 1(a)



(a) 3D microstructure of 304L stainless steel obtained from DCT



(b) Inverse pole figure of the sample regarding to some macroscopic directions r

Figure 1: Experimental characterization of the material

where each color is linked to a specific crystallographic orientation. For this kind of material, the mechanical anisotropy can be associated to several sources. First, each single crystal presents an anisotropic behavior which can be described by a cubic tensor in the elastic domain. The anisotropy of the polycrystalline aggregate is of course connected to the orientation of each single crystal and to the shape of the constituant. Former studies suggest that the overall anisotropy is mainly connected to the local anisotropy caracterized by Zener's parameter and to the texture of the material at least in the elastic domain. Nevertheless, the details of the mechanical fields can be affected by others microstructural features. To determine the orientation distribution function (ODF) from EBSD measurements, the harmonic method, which consists in a serie expansion of the ODF on a basis of spherical harmonic functions, has been used. The figure 1(b) shows the inverse pole figure of the austenite. It can be seen that the material exhibit a strong fiber texture in the $< 111 >$ direction and a slightly less pronounced fiber in the $< 001 >$. The overall behaviour is thus expected to present a symmetry close to transverse isotropy.

3. Numerical homogeneization using FFT

The DCT data can be used as microstructural inputs for a micromechanical modelling scheme. As noted previously, the widely used FE technique implies a complex task of meshing for a careful description of grain boundaries and, on the opposite, the use of a simple cartesian mesh is known to have a poor numerical efficiency regarding to dedicated algorithms on this topology. Consequently, we have chosen an alternative approach to treat this problem at reduced computational cost (problems with several millions of degrees of freedom can be solved in a few minutes with this technique [11]). Also, an attractive feature is that the image of the microstructure can be used directly as an input without using dedicated meshing algorithm. The principle is based on the fact that the local mechanical response of a periodic heterogeneous medium, discretized on a $N_x \times N_y \times N_z$ unit cell, can be computed as a integral equation. This operation convolves the Green's function of a linear reference homogeneous medium with the actual heterogeneity field, called polarization field $\boldsymbol{\tau}(\boldsymbol{x})$. This description of the problem is similar to numerous treatments encountered in homogenization theory [12, 13] where the initial heterogeneous problem is replaced by an equivalent homogeneous problem with polarization :

$$\boldsymbol{\sigma}(\boldsymbol{x}) = \boldsymbol{C}(\boldsymbol{x}) : \boldsymbol{\varepsilon}(\boldsymbol{x}) \quad \text{becomes} \quad \boldsymbol{\sigma}(\boldsymbol{x}) = \boldsymbol{C}^0 : \boldsymbol{\varepsilon}(\boldsymbol{x}) + \boldsymbol{\tau}(\boldsymbol{x}) \text{ with } \boldsymbol{\tau}(\boldsymbol{x}) = \left(\boldsymbol{C}(\boldsymbol{x}) - \boldsymbol{C}^0\right) : \boldsymbol{\varepsilon} \tag{1}$$

If the convolution problem is difficult to solve in the real space its counterpart in the Fourier space is only a simple tensorial product. This observation has motivated the use of an algorithm based on Fast Fourier Transform (FFT) to solve this unit cell problem [10]. In the following, the integration algorithm which follows the proposal of [14] is described hereafter. Note that the plastic slip increments $\Delta\gamma^{k^\star}$ are computed by randomly chosing a set of linearly independent and potentially active slip systems. The consistency condition delivers a relation between $\Delta\gamma^{k^\star}$ and the increment of total strain $\Delta\boldsymbol{\varepsilon}$.

4. Results and discussions

4.1. Young's modulus of the aggregate

In order to describe the elastic anisotropy of the overall behavior of the material, the directional dependence of Young's modulus E is computed with

$$\frac{1}{E(\boldsymbol{n})} = \left(\boldsymbol{n} \otimes \boldsymbol{n} : \widetilde{\boldsymbol{S}} : \boldsymbol{n} \otimes \boldsymbol{n}\right) \tag{2}$$

Algorithm 1 Rate independent elastoplastic behaviour

$\boldsymbol{\sigma}_n = \mathrm{g}(\boldsymbol{\varepsilon}_n)$

- strain field $\boldsymbol{\varepsilon}_n(\boldsymbol{x}_g)$ known, $\forall\, \boldsymbol{x}_g$
- elastic guess : $\boldsymbol{\sigma}^E = \boldsymbol{\sigma}_{n-1} + \boldsymbol{C} : (\boldsymbol{\varepsilon}_n - \boldsymbol{\varepsilon}_{n-1})$
- resolved shear stresses : $\tau^k = \boldsymbol{\mu}^k : \boldsymbol{\sigma}^E,\ \forall k$
- plastic criterion (Schmid law)

if $\tau^k < \tau^k_{cn-1},\ \forall k$ **then**

$\boldsymbol{\sigma}_n = \boldsymbol{\sigma}^E, \quad \Delta\tau^k_c = 0$

else

- consistency condition : $\Delta\tau^{k^\star} = \Delta\tau^{k^\star}_c \Rightarrow \Delta\gamma^{k^\star},\ k^\star \in \mathcal{K}^\star$

$\mathcal{K}^\star$ = set of potentially active slip systems

- plastic strain increment : $\Delta\boldsymbol{\varepsilon}^{\mathrm{P}} = \sum_{k^\star} \boldsymbol{\mu}^{k^\star} \Delta\gamma^{k^\star}$
- elastoplastic guess : $\boldsymbol{\sigma}_n = \boldsymbol{\sigma}^E - \boldsymbol{C} : \Delta\boldsymbol{\varepsilon}^{\mathrm{P}}$
- critical shear stresses increment : $\Delta\tau^k_c = \sum_{k^\star} h^{kk^\star} \Delta\gamma^{k^\star}$

end if

where $\boldsymbol{n}$ is the direction of uniaxial tension. The elastic moduli characterizing the full effective response have been obtained by performing six FFT computations with independent macroscopic loadings. The effective Young's modulus obtained by FFT can be compared to results derived from analytical homogenization models, namely the self-consistent (SC) scheme and Voigt and Reuss bounds [12]. The effective tensors for these different models are given by

$$\widetilde{\boldsymbol{C}}_{\mathrm{Voigt}} = \langle \boldsymbol{C} \rangle\,, \qquad (\widetilde{\boldsymbol{C}}_{\mathrm{SC}} + \boldsymbol{C}^*)^{-1} = \left\langle (\boldsymbol{C} + \boldsymbol{C}^*)^{-1} \right\rangle, \qquad \widetilde{\boldsymbol{S}}_{\mathrm{Reuss}} = \langle \boldsymbol{S} \rangle\,. \tag{3}$$

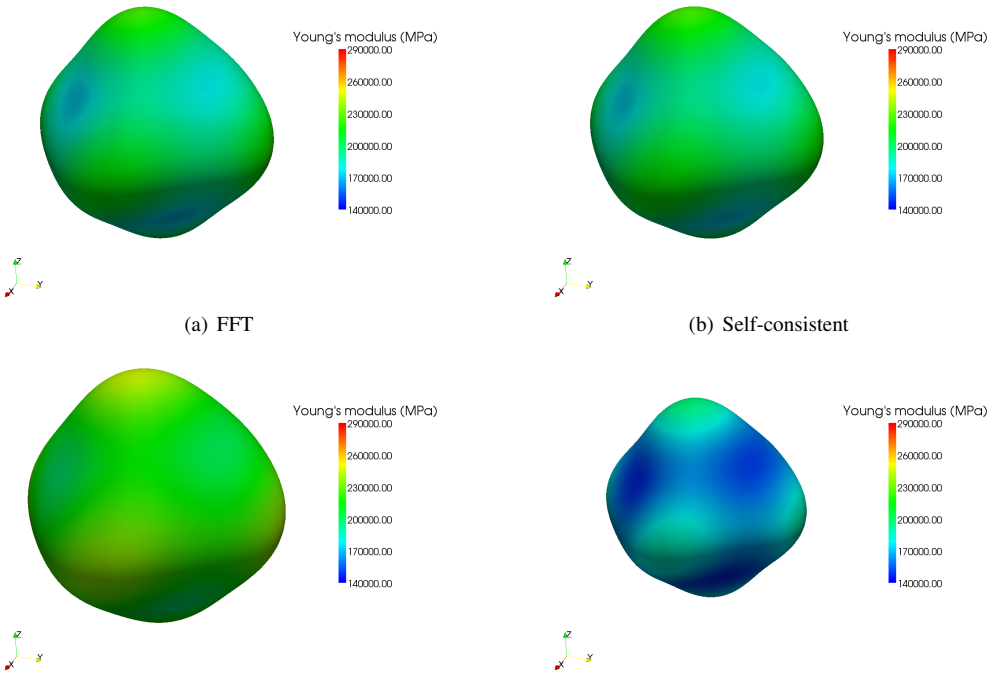
where $\langle . \rangle$ represents spatial average and $\boldsymbol{C}^*$ is the "constraint tensor" introduced by Hill [13]. The results obtained are presented on figure 2. The different figures present a very similar evolution with respect to the loading direction since crystallographic texture is the first order microstructural parameter, and it is verified that the FFT and SC results is bounded by the Voigt and Reuss estimates. The obtained highest stiffness along the macroscopic z axis is consistent with the strong $< 111 >$ fiber texture and the anisotropy of the single crystal of austenite. Interestingly, the self-consistent estimate is very close to the "exact" response obtained by FFT which takes into account the shape and spatial distribution of the individual grains in the 3D austenite sample.

4.2. Elastoplastic response and spatial distribution of the local fields

The plastic deformation occurs by glide on octahedral slip systems $\{111\} < 110 >$ and the critical resolved shear stresses are constant. Figure 3 shows the uniaxial tensile response of this aggregate and the distribution of deformation ε_{33} in the plastic regime. The presence of shear bands at +/- 45° spreading over many grains can be noticed. These results are in agreement with experimental observations [15] and modelling results by FE [16].

5. Concluding remarks

In this work, DCT data have been used to compute, with a FFT numerical scheme, the effective properties and local mechanical fields of a 3D microstructure of austenitic steel. The results are found to be in good agreement with the self-consistent estimate, at least in the elastic



(a) FFT (b) Self-consistent

(c) Voigt (d) Reuss

Figure 2: Directional variation of Young's modulus for different homogenization models.

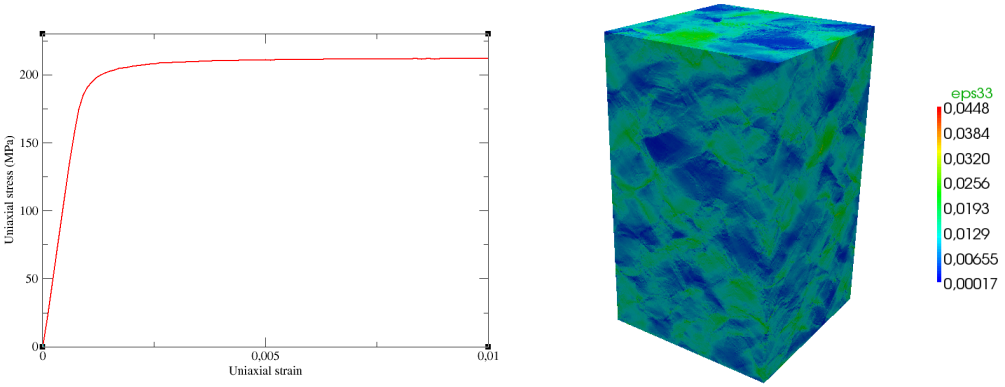


Figure 3: Overall stress-strain curve of the material for unixial tensile test (on the left), spatial distribution of the ε_{33} field at 1% overall strain (on the right).

regime, and are consistent with previous simulations and observations concerning strain localization in the plastic regime. On-going works are concerned by the implementation of more advanced constitutive relations using dislocation densities as internal variables and comparisons with other modelling approaches, namely non-linear mean field homogenization scheme and FE computations.

[1] A. Schwartz, M. Kumar, B. L. Adams, D. P. Field (Eds.), Electron Backscatter Diffraction in Materials Science, Springer, 2000.

[2] B. Adams, T. Olson, The mesostructure–properties linkage in polycrystals, Prog. Mater. Sci. 43 (1) (1998) 1 – 87.

[3] R. A. Lebensohn, R. Brenner, O. Castelnau, A. D. Rollett, Orientation image-based micromechanical modelling of subgrain texture evolution in polycrystalline copper, Acta Mater. 56 (2008) 3914–3926.

[4] L. St-Pierre, E. Héripré, M. Dexet, J. Crépin, G. Bertolino, N. Bilger, 3d simulations of microstructure and comparison with experimental microstructure coming from o.i.m analysis, Int. J. Plasticity 24 (9) (2008) 1516 – 1532.

[5] A. Zeghadi, S. Forest, A. Gourgues, O. Bouaziz, Ensemble averaging stress-strain fields in polycrystalline aggregates with a constrained surface – part 2: crystal plasticity.

[6] D. Rowenhorst, A. Gupta, C. Feng, G. Spanos, 3d crystallographic and morphological analysis of coarse martensite: Combining ebsd and serial sectioning, Scripta Mater. 55 (1) (2006) 11 – 16.

[7] T. Matteson, S. W. Schwarz, E. Houge, B. Kempshall, L. Giannuzzi, Electron backscattering diffraction investigation of focused ion beam surfaces, J. Electron. Mater. 31 (1) (2002) 33 – 39.

[8] G. Johnson, A. King, M. Honnick, J. Marrow, W. Ludwig, X-ray diffraction contrast tomography: A novel technique for three-dimensional grain mapping of polycrystals, J. Appl. Cryst. 41 (2008) 310–318.

[9] W. Ludwig, A. King, P. Reischig, M. Herbig, E. Lauridsen, S. Schmidt, H. Proudhon, S. Forest, P. Cloetens, S. R. du Roscoat, J. Buffière, T. Marrow, H. Poulsen, New opportunities for 3d materials science of polycrystalline materials at the micrometre lengthscale by combined use of x-ray diffraction and x-ray imaging, Mater. Sci. Eng. A 524 (2009) 69 – 76.

[10] H. Moulinec, P. Suquet, A numerical method for computing the overall response of nonlinear composites with complex microstructure, Comput. Methods Appl. Mech. Engrg. 157 (1-2) (1998) 69 – 94.

[11] J. Michel, H. Moulinec, P. Suquet, Effective properties of composite materials with periodic microstructure: a computational approach, Comput. Methods Appl. Mech. Engrg. 172 (1-4) (1999) 109 – 143.

[12] J. Willis, Variational and related methods for the overall properties of composites, Vol. 21, Elsevier, 1981, pp. 1 – 78.

[13] R. Hill, Continuum micro-mechanics of elastoplastic polycrystals, J. Mech. Phys. Solids 13 (2) (1965) 89 – 101.

[14] J. W. Hutchinson, Elastic-plastic behaviour of polycrystalline metals and composites, Proc. R. Soc. Lond. A 319 (1970) 247–272.

[15] P. Doumalin, Microextensométrie locale par corrélation d'images numériques, Ph.D. thesis, Ecole Polytechnique (2000).

[16] F. Barbe, R. Quey, A. Musienko, G. Cailletaud, Three-dimensional characterization of strain localization bands in high-resolution elastoplastic polycrystals, Mech. Res. Commun. 36 (2009) 762–768.